

Research Journal of Pharmaceutical, Biological and Chemical Sciences

Topical Nitric oxide in nanoformulation enhanced wound healing in experimental diabetes in mice.

Rovan Samaha^{1*}, Azza I Othman¹, Ibrahim M. El-Sherbiny², Maher A Amer¹, Fatma Elhousseini³, Mohamed A ElMissiry¹, Ali H Amin¹, and Mohamed Ahdy A.A. Saad⁴.

¹Zoology Department, Faculty of Science, Mansoura University, Mansoura, Egypt.

²Center for Materials Science, Zewail City of Science and Technology, 6th October City, Giza, Egypt.

³Pathology Department, Faculty of Medicine, Mansoura University, Mansoura, Egypt.

⁴Pharmacology Department, Faculty of Medicine, Mansoura University, Mansoura, Egypt.

ABSTRACT

Chronic diabetes with uncontrolled hyperglycemia is associated with impaired wound healing due to increased oxidative stress and low nitric oxide (NO) level in wound tissue. Nanotechnology enables synthesizing nanoparticle with efficient drug delivery. The aim of the present study was to evaluate bandage formulated with nitric oxide donor nanoparticles (NONPs) on wound healing in STZ-induced DM in mice. In the present study nitric NONPs was prepared as powder size ranging from 19-28 nm and mixed with vaseline to form cream bandaged for topical application. Two excisional wounds were made on the dorsa of mice. The present results demonstrated significantly enhanced healing after 7 and 14 days from induction of the wound. Compared to diabetic mice, wound tissue showed increased levels of NO and GSH, upregulated activities of SOD and CAT and decreased MDA content. Topical application of NONPs bandage improved wound vascularization evidenced histologically and by significantly increased vascular endothelial growth factor (VEGF) and transforming growth factor β 1 (TGF- β 1) in serum. The present results emphasize the potential of a new nitric oxide platform for wound healing therapy.

Keywords: Nitric oxide, nanoformulation, wound healing, diabetes.

**Corresponding author*

INTRODUCTION

Impaired wound healing is a major concern and problem for diabetic patients. The number of diabetic patients are increasing and might reach 400 million on 2025 [1]. It is estimated that 25% of diabetic patients usually exhibit foot ulceration and impaired wound healing [2]. The diabetic wound complication is associated with impaired vascularization, prolonged inflammation, augmented oxidative stress and poor oxygen and nutrient supply leading to intractable wounds [3].

The impairment of wound healing is also associated with reduced synthesis and bioavailability of nitric oxide (NO) due to vascular endothelial dysfunction in diabetics [4]. NO is an intrinsic cellular signaling molecule for normal wound healing [5]. Reduced levels of NO in the wound milieu can lead to vasoconstriction, an altered vascular redox state, abnormal growth of vascular smooth muscle cells, and prothrombotic changes in the vessel wall which leads to poor wound healing process [6]. Recently it is reported that NO containing compounds such as nitroglycerine (isosorbide dinitrate) and arginine silicate inositol complex [7, 8] are shown to enhance wound healing as topical treatment in diabetic animal models.

Nanotechnology and nanoparticles (NPs) production is the most recent trend and effective therapeutics in last 20 years due to their low toxicity and physiochemical properties [9]. Since the fundamentals of most biological processes and mechanisms occur at nanometer scale, NPs can offer a successful platform for drug delivery [10]. In the context of enhancing cutaneous wound healing, several NP-based therapeutics that employed for clinical and undergoing preclinical trials include metals, antibiotics, natural products, lipid based, polymer based-NPs and nitric oxide releasing NPs, are recently reported [9, 11]. The last modality enables exogenous supply of NO in the microenvironment of the wound [11].

Because diabetic wound closure can be hampered by decreased production of NO in the wound microenvironment, we hypothesized that NO supplementation would enhance wound healing by restoring NO synthesis. However, this approach has been limited by the short duration of NO release, short half-life of NO, and instability of available NO donors [12]. To overcome these deficiencies, we have developed a new nitric oxide donor nanoparticles (NONPs) powder made from sodium nitrite as NO delivery platform. Therefore, the aim of the present study was to evaluate a bandage formulated with NONPs on an excisional wound model in STZ-induced DM in mice.

MATERIALS AND METHODS

Chemicals

Streptozotocin (STZ), Tetramethoxyorthosilicate (TMOS), Polyethylene glycol, Phosphate-buffered saline (PBS) pH 7.5, Chitosan and Sodium nitrite were purchased from Sigma Aldrich Co. (St. Louis, MO 6, USA).

Experimental animals

Adult male BALB-C mice weighing 30-35 g raised at Medical experimental research center (MERC), faculty of medicine, Mansoura university were kept under good ventilation; adequate stable diet and were allowed to ad libitum.

Methods

Preparation of NO-releasing hydrogel nanoparticles

NO-releasing hydrogel nanoparticles were prepared through a method adapted from [13] with some modifications. Briefly, 5 ml of TMOS were mixed with HCl solution (560 μ l of 0.2 mM HCl added to 600 μ l of deionized water) followed by immediate sonication for 45 minutes in a cold water bath. Then, the sonicated mixture (A) was placed onto a few grams of ice. Afterwards, 1.8 gm of sodium nitrite was dissolved in 100 ml of 50 mM PBS (pH 7.5) followed by addition of 40 mg of D-glucose and 1ml PEG/20 ml of buffer solution with stirring to produce the 1ry buffered solution. In another beaker, a solution of 5 mg chitosan/ ml of acidified distilled water (0.5% acetic acid) were prepared followed by addition of 1ml of this mixture to 20 ml of the 1ry buffered solution prepared earlier with stirring to form the final buffered solution. TMOS mixture (A) was then

introduced slowly to the final buffered solution in a ratio of 2 ml TMOS/20 ml buffer with immediate stirring and the resulting mixture was set aside. This mixture undergoes gelation within 1-2 hours which is then brought out from the container and crudely dried by blotting with paper towel. Three drying methods (air drying, heating and lyophilization) were then applied for the resulting sol-gel blocks. The final obtained nanoparticles were stored until further investigation, and the lyophilized nanoparticles were in a good powder form and used in the rest of experiments.

Characterization of the NO-releasing nanoparticles

The developed NO-releasing hydrogel nanoparticles were characterized using different analytical techniques. FTIR measurements were carried out using NECOLET iS10-attenuated total reflectance, ATR-FTIR spectroscopy (NECOLET iS10, Thermo Fisher Scientific, US) to confirm the structure of the resulting nanoparticles. Samples were placed on a KBr diamond and the measurements were carried out in the range of 400–4000 cm^{-1} at a resolution of 2 cm^{-1} . The size of the prepared NO-releasing nanoparticles was measured using dynamic light scattering, DLS (Malvern nanosizer, Malvern Instruments Ltd., Worcestershire, UK). The morphology of the prepared nanoparticles was investigated by high resolution transmission electron microscopy, TEM (Joel-100 CX, Japan) at the Electron Microscope Unit, Faculty of Science, Alexandria University, Alexandria, Egypt. The TEM was attached to a CCD camera at an accelerating voltage of 200 kV. The specimens were prepared via placing the NO-nanoparticles powder on a carbon coated copper grid followed by capturing the TEM images.

Release profile of NO from the prepared hydrogel nanoparticles

The released NO from the developed hydrogel nanoparticles was measured using a NO electrode where two concentrations of the NO-eluting nanoparticles (2.5 and 5 mg/ml) were prepared in PBS (7.1) and measured over a period of 80 min.

Induction of experimental Diabetes

Diabetes mellitus was induced by a single intraperitoneal injection of 120 mg/kg bw STZ dissolved in citrate buffer pH 4.5. STZ-treated mice were given 5% glucose to counter any initial hypoglycemia. Hyperglycemia was confirmed by blood glucose test. Mice with fasting blood glucose level $\geq 250\text{mg/dl}$ were used for the study. Glucose levels were measured by a one-touch blood glucose meter (Life- Scan Inc., Milpitas, USA) from the tail vein. Animal experiments were performed in accordance with the Declaration of Helsinki under the protocol approved by the Animal Research Committee at Mansoura University.

Induction of experimental wound model:

Full thickness excisional wounds were made on the back of the mouse as previously described [1]. Briefly, the mice were anesthetized with mixture of 0.05 ml valium and 0.1 ml Ketamin and the backs of all mice were shaved then sterilized by 70% (v/v) ethanol. The full thickness two excisional wounds were made on the folded skin by a sterile biopsy punch. To avoid self-licking the yielded two wounds were mad on the dorsum between the shoulder blades of each mouse.

Animal grouping: Animals were divided into the following 4 groups 18 animal in each group.

- a) Non-diabetic wounded control mice were ip injected vehicle. Wounds were made then covered with void cotton bandage.
- b) Non-diabetic wounded control mice were ip injected vehicle. Wounds were made and covered with NONPs bandages.
- c) Diabetic wounded mice received a single ip STZ (120mg/kg b.w) then wounded. Wounds were covered by void cotton bandages.
- d) Diabetic wounded mice received a single ip STZ (120mg/kg b.w) and wounded. Wounds covered with NONPs bandages.

Sampling and wounding

At the end of experimental periods on the 3rd, 7th and 14th day after wounding overnight fasted mice were anesthetized using single intraperitoneal injection of thiopental then sacrificed. Blood samples were collected in clean centrifuge tubes then centrifuged at 3000 rpm for 15 min. Blood sera were carefully separated and kept at -20°C for glucose determination.

Skin specimens were quickly removed including the whole wounds and the healthy edges around each wound. One of the two wounds were homogenized in cold PBS to form 10% (w/v) homogenate for biochemical assays and kept at -20°C and the other were kept in neutral buffer formalin for pathological investigations.

Measurement of wound closure area

Wounds in each individual mouse were photographed digitally every day, beginning on the day of wounding day 0, 3, 7, & 14. The quantification of Wound closure was quantified as previously described [1]. The area of wound closure was expressed as cm^2 (each day after wounding) compared to the initial wound area. A smaller wound area indicated faster wound closure.

Determination of glucose concentration in serum: The concentration of glucose in serum was estimated by the method of [14] by using SPINREACT diagnostics kit, Spain.

Determination of wound nitric oxide concentration. The concentration of wound nitric oxide was estimated by the method of [15] by using Biodiagnostic kit, Egypt.

Determination of wound malondialdehyde (MDA):- The amount of malondialdehyde (MDA) was measured by the thiobarbituric acid assay which is based on MDA reaction with thiobarbituric acid to give a red color measured at 535 nm [16].

Determination of wound glutathione (GSH) content:- This method depends on the precipitation of protein using tungstate/sulfuric acid solution and the formation of yellow color after reaction with 5, 5-dithiobis-25-nitrobenzoic acid (DTNB) and read at wavelength 412 nm [17].

Determination of wound superoxide dismutase (SOD) activity: SOD activity was assayed by the procedure as previously reported [18]. The assay relies on the ability of the enzyme to inhibit phenazine methosulphate mediated reaction of nitroblue tetrazolium dye.

Determination of wound catalase (CAT) activity:- Catalase activity was determined by the method as described previously [19]. The decomposition of H_2O_2 can be followed directly by the decrease in the absorbance at 240 nm. The difference in the absorbance per unit time is a measure of the CAT activity.

Determination of wound vascular endothelial growth factor (VEGF). Determination of wound VEGF was determined by the method of [20] by using Boster immunoleader assay kit, USA.

Determination of wound Transforming Growth factor β (TGF- β). Determination of wound TGF- β was determined by the method of [21] by using Boster immunoleader assay kit, USA.

Histopathological examination. Wound specimens which were fixed in 10% neutral buffered formalin were allowed for dehydration then embedded in paraffin, and finally stained with hematoxylin-eosin and Masson's trichrome stains by the method of [22].

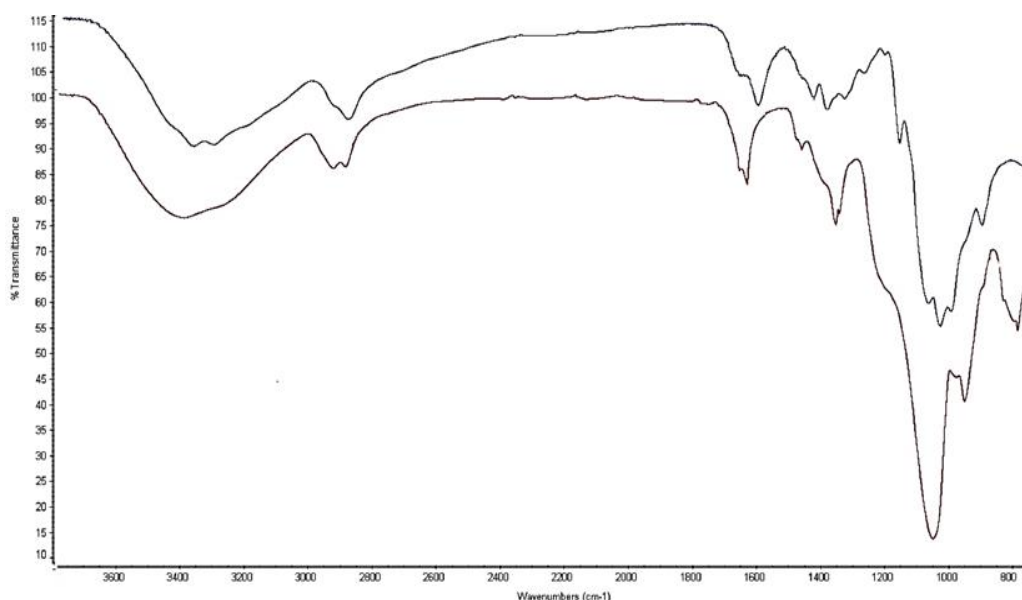
Statistical analysis: Statistical analysis was performed using MINITAB for Windows statistical package (Version 13) 2001. All results were calculated as the percentage of mean control values. Group results were then expressed as mean \pm the standard error of the mean (SEM). Statistical differences from control were determined using one way analysis of variance with a Dunnett correction for multiple comparisons and significance was calculated as $p \leq 0.05$.

RESULTS

Characterization of the NO-releasing nanoparticles

The prepared NO-releasing nanoparticles were characterized using various analytical techniques. FTIR spectra of the developed nanoparticles in comparison to its basic polymeric component, chitosan was obtained as shown in Figure 1. As can be noted from the figure, the chitosan IR spectrum demonstrated a peak at about 3342 cm^{-1} which was assigned for the N-H extension vibration, the O-H stretching vibration, and the H-bonding of the polysaccharide moieties of the chitosan polymer. The peak noted at 2883 cm^{-1} was assigned for the stretching vibrations of the C-H (aliphatic) bonds whereas, the absorption signal noted at 1590 cm^{-1} was attributed to the stretching vibration of amide C=O bonds. The prepared NO nanoparticle showed a similar IR spectrum to that observed for chitosan with a minor shift in some of the IR absorption peaks. The nanoparticles were also characterized using HR-TEM microscopy (Figure 2a). As shown in the figure, the developed NO-releasing nanoparticles are spherical with a particle size of mostly less than 50 nm.

Figure 1: FTIR spectrum of the developed NO-releasing nanoparticles as compared to that of chitosan.



The average size of the prepared NO-nanoparticles was also determined using DLS as apparent from Figure 2b. As apparent from the figure, most of the nanoparticles showed a size less than 40 nm, in agreement with the TEM micrographs, with some of the particles aggregated up to a size of 200 nm. When analyzed using powder X-ray diffraction (Figure 2c), the NO-releasing nanoparticles depicted a peak at 23.4° and spikes consistent with some level of crystalline structure.

The release profile of NO from the developed nanoparticles is shown in Figure 3. As apparent from the figure, there was an immediate release of NO upon the addition of the hydrogel nanoparticles to the PBS buffer. Then, a gradual increase in the released NO was noted over the investigated time. Increasing the initial concentration of the nanoparticles demonstrated a significant increase in the released NO (nM) at any time interval.

The size of the NONPs was determined by TEM and ranged from 19 nm to 28 nm as shown in Figure 2a. The TEM micrographs also showed a spherical morphology of the NO-nanoparticles.

Figure 2: Characterization of nitric oxide releasing nanoparticles. (a) Transmission electron micrograph, (b) Particle size analysis as determined by DLS showing a spherical morphology and (c) X-ray diffraction of the developed NO-releasing nanoparticles

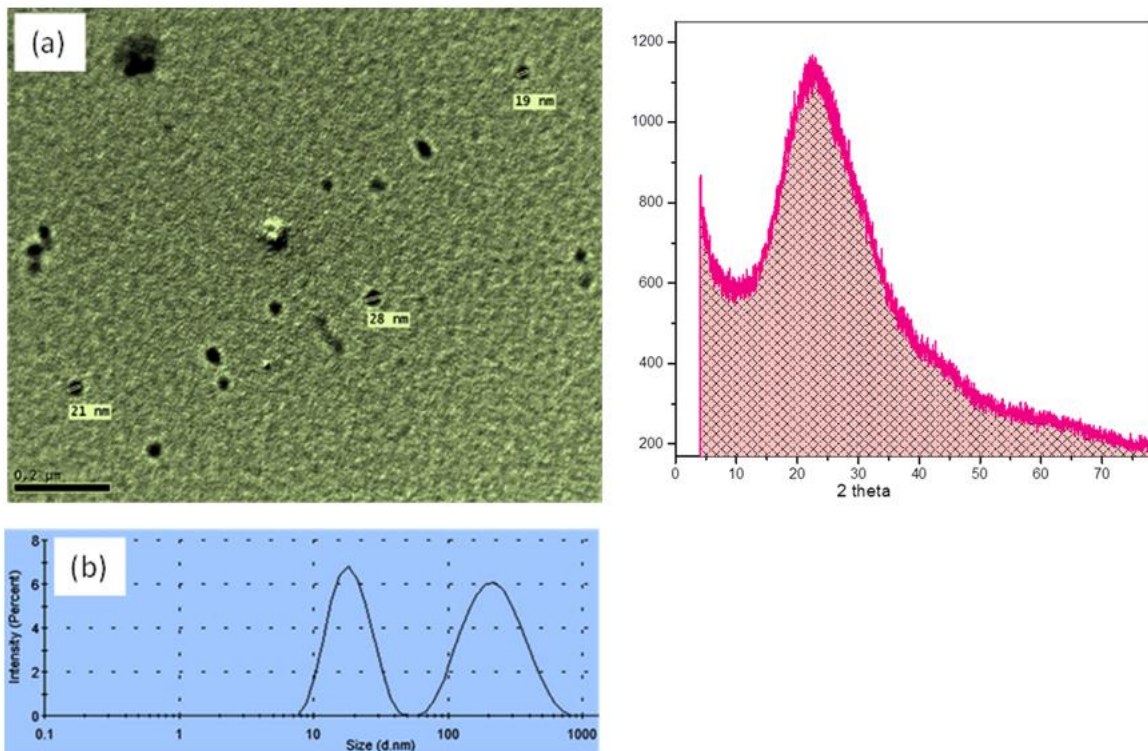
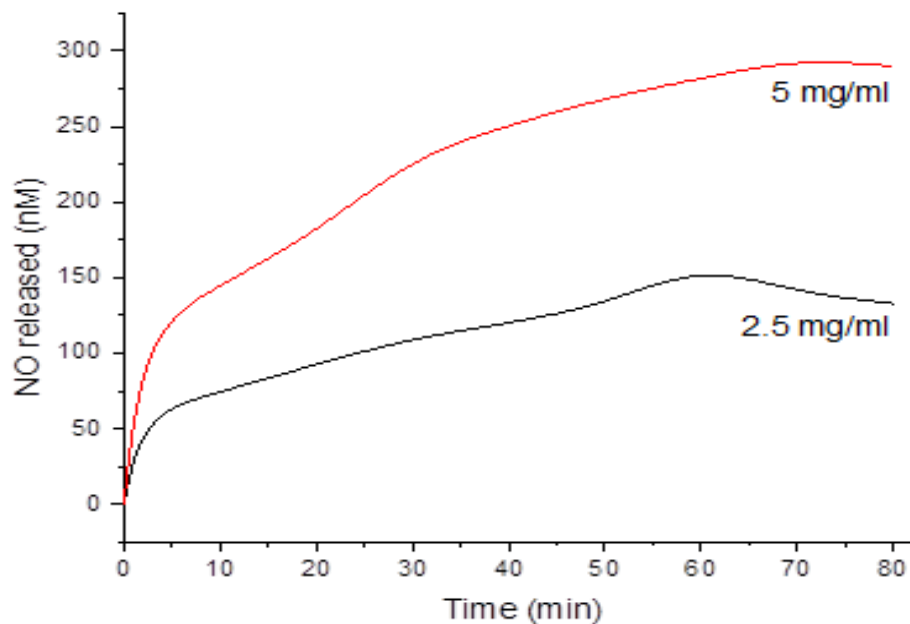


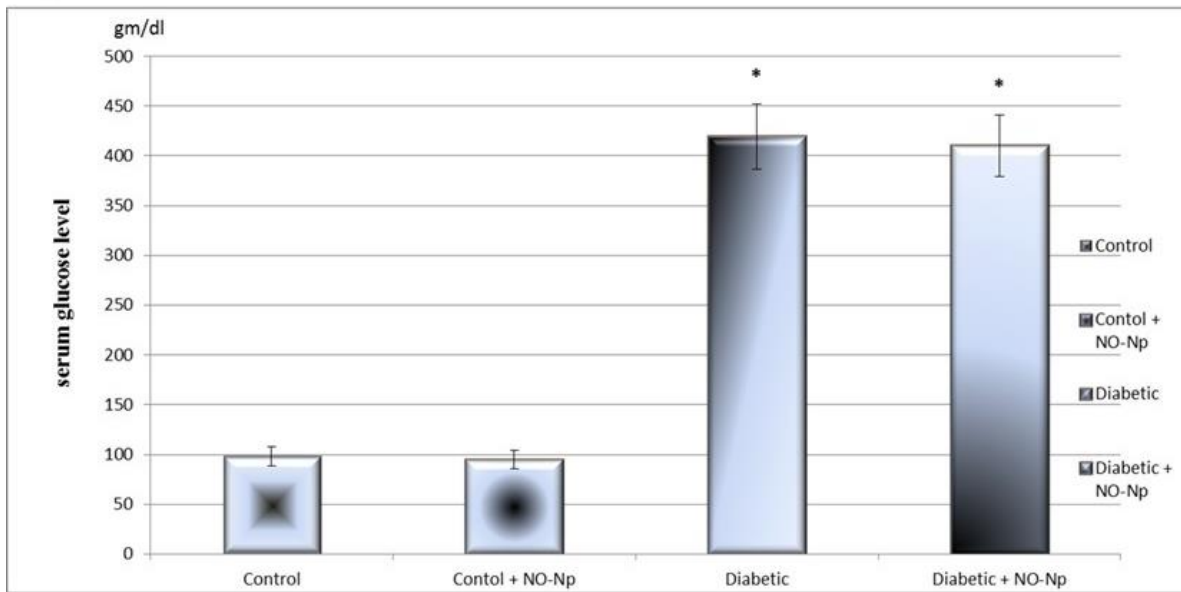
Figure 3: Release profile of NO from the prepared hydrogel nanoparticles.



Biochemical investigations

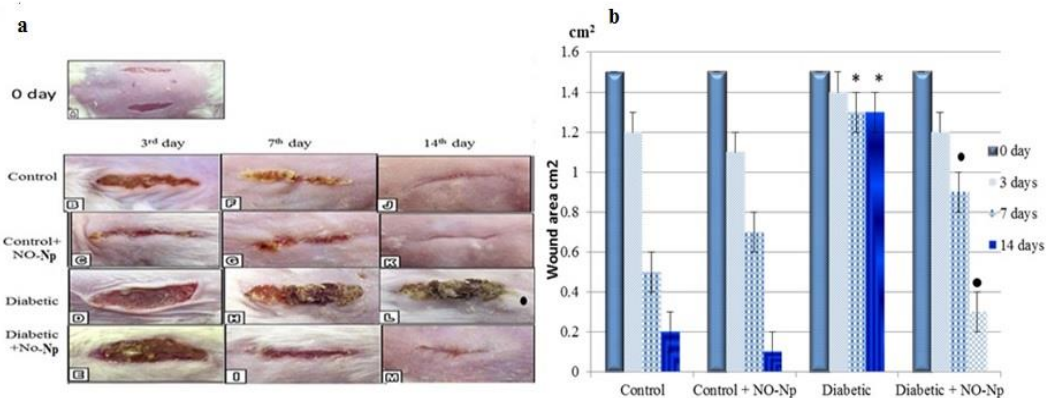
The blood glucose of the diabetic mice significantly increased during the experimental period compared to that of the control group. The diabetic mice treated with NONPs bandage also exhibited a marked elevation of blood glucose over the experimental period similar to diabetic group and significantly higher than the control groups (Figure 4).

Figure 4: Levels of serum glucose in different animal groups



The wound closure area of the diabetic animals significantly delayed from day 3 as compared to those of the control group. However, the wound closure of the NONPs-treated group was accelerated significantly from day 3 as compared to those of the diabetic group (Figure 5 a&b).

Figure 5: Effect of topical application of NO-releasing nanoparticles (NONPs) on healing of wound in diabetic mice compared with control group, (a) A representative image of mouse from each group taken on post-injury days 3, 7 and 14. Topical application of NONPs on wound of diabetic mice markedly accelerated the wound healing compared with diabetic mice. (b) Wound area at the indicated time points in and control and topically treated mice (n = 6). The cutaneous wound area significantly decreased in NONPs treated diabetic mice compared with diabetic group.



In wound tissue of diabetic animals there were significant decreases GSH and NO levels and the activity of SOD and CAT with concomitant elevation of MDA content. On the other hand, when wound covered with NONPs bandage, oxidative stress was ameliorated evidenced by lower level of MDA with higher concentration of GSH and NO as well as the activities of SOD and CAT compared to diabetic mice.

The levels of the VEGF and TGF-B1 were significantly down regulated in the serum of the diabetic animals. NONPs bandage application on diabetic wound ameliorated the decline in these growth factors in the serum and displayed insignificant changes when compared to the control rats. Compared to the diabetic animals, VEGF levels were increased in day 7 and 14 in serum after application of NONPs on wound of the diabetic animals. Similarly TGF-B1 showed comparable trend in day 14.

Figure 6: (a)Effect of topical treatment of nitric oxide-releasing nanoparticles on the level of wound nitric oxide, (b): wound malondialdehyde (MDA) content (nM/mg wt tissue), (c): glutathione (GSH) content (mg/g wt tissue), (d): superoxide dismutase (SOD) activity (U/g wt tissue) and (e): (CAT) activity ($\mu\text{M H}_2\text{O}_2/\text{sec/g wt tissue}$) in control and different animal groups at 3,7, and 14 days of wounding .

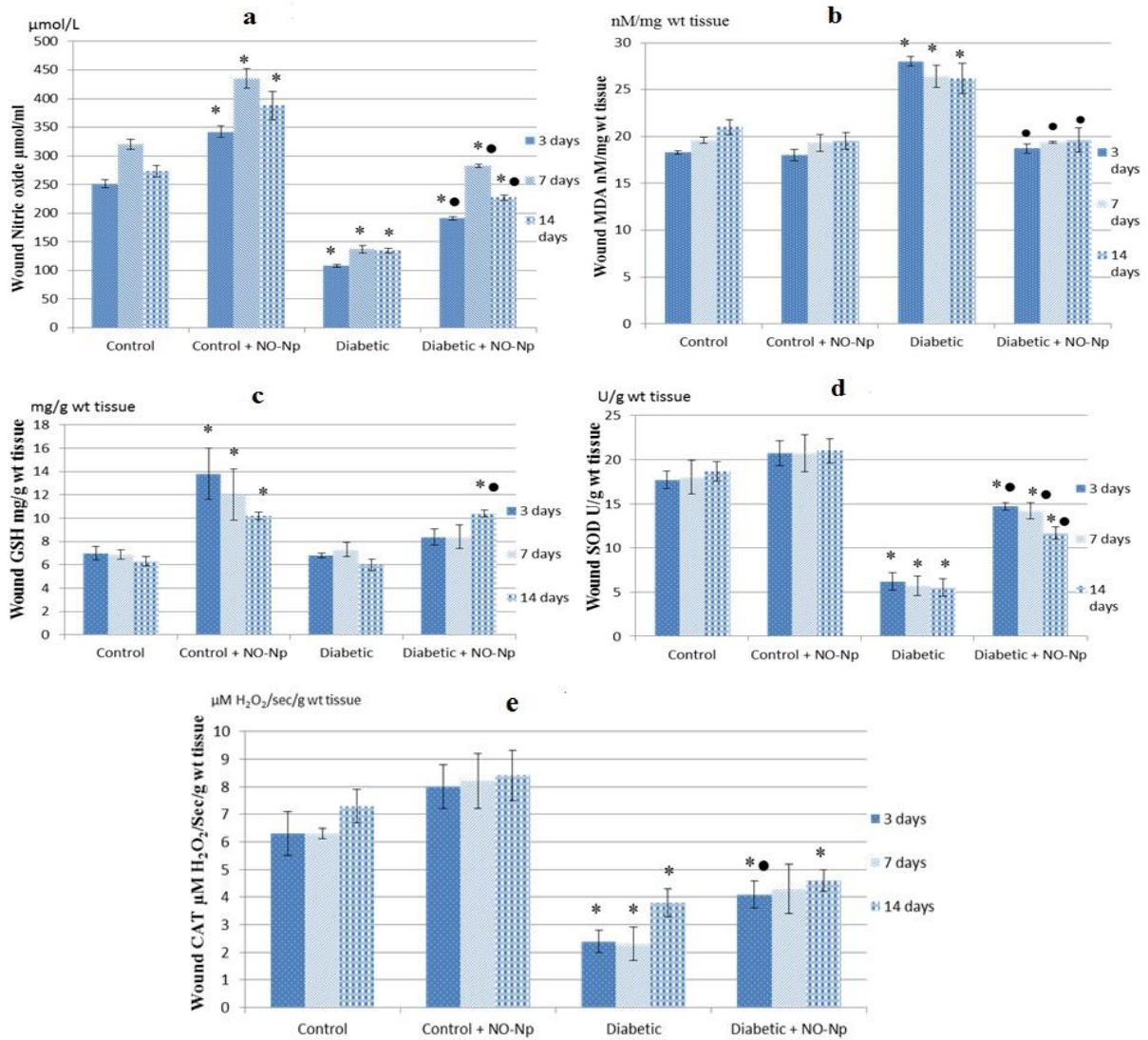
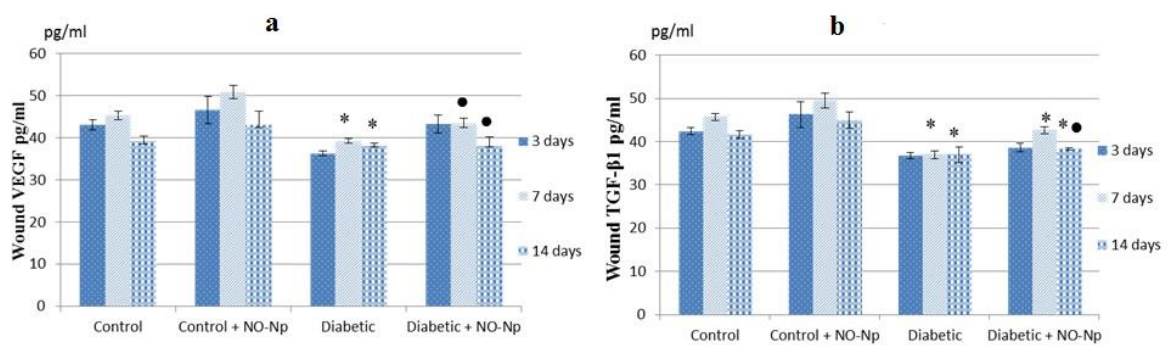


Figure 7: (a)Effect of topical treatment of nitric oxide-releasing nanoparticles on the vascular endothelial growth factor (VEGF) concentration (pg/ml) and (b): transforming growth factor- β 1 (TGF- β 1) Concentration (pg/ml) in the cutaneous wound tissue in control and different animal groups at 3,7, and 14 days of wounding at 3, 7, and 14 days after injury.



Histopathological Observations:

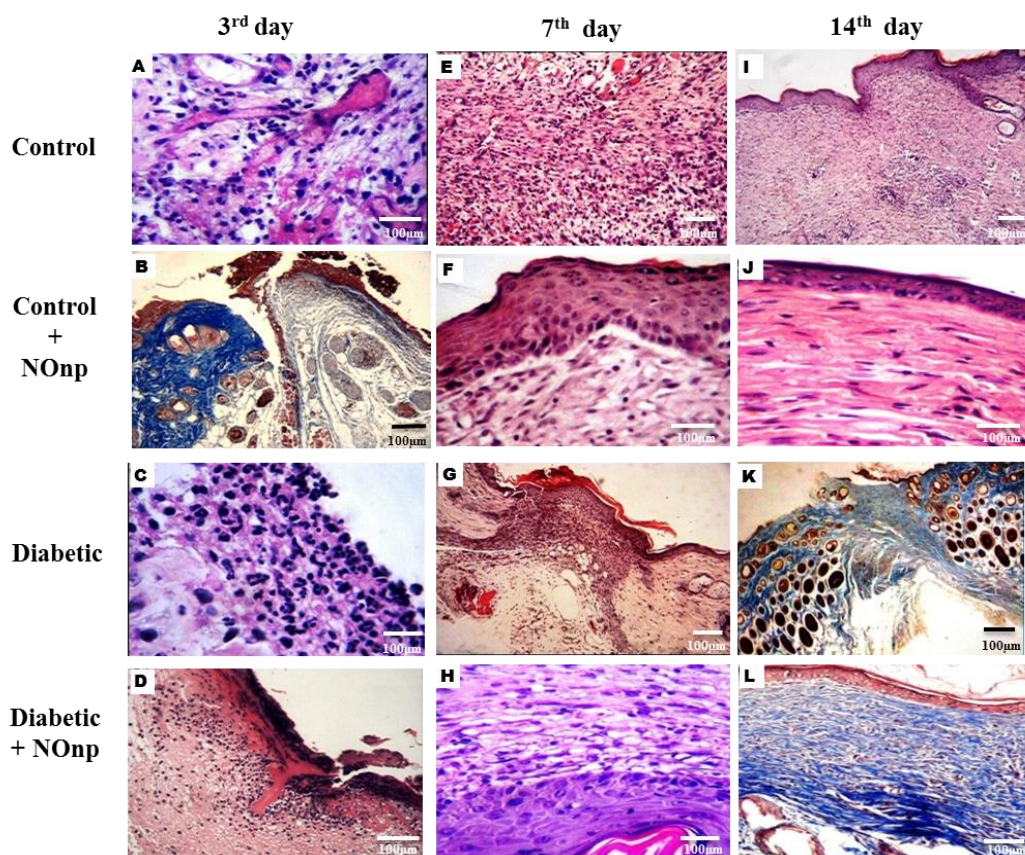
Fig (8) Histopathological observations of the wound after 3, 7 and 14 days of wound induction in control group and different treated animal groups were illustrated in figure 8 A-L.

Figure 8A shows neovascularization extension from capillaries in control group after 3 days of wound induction. Fig 8B illustrate deep loose fibrous tissue extending with its nerve bundles to line the lateral borders of the wound control group received NONPs after 3 days of wound induction. Figure 8C display neutrophil infiltration of the surface epithelial in diabetic group after 3 days of wound induction. Figure 8D demonstrates necrotic tissue in the wound with neutrophils in diabetic group received NONPs after 3 days of wound induction.

Figure 8E shows lateral side of the wound with nerve bundles in control group after 7 days of wound induction. Figure 8F depicts regenerating surface epithelium without hair follicles in control group received nitric oxide donor nanoparticles after 7 days of wound induction. Figure 8G illustrate scar tissue pulling upward the subcutaneous fat and underlying fibrous tissue in diabetic group after 7 days of wound induction. Figure 8H shows newly formed capillaries in regenerating epithelium in diabetic group received NONPs after 7 days of wound induction.

Figure 8I represents regenerating epithelium over the scar in control group after 14 days of wound induction. Figure 8J displays surface epithelium flat overlying scar tissue in control group received nitric oxide donor nanoparticles after 14 days of wound induction. Figure 8K demonstrates scar tissue between two healthy edges in diabetic group after 14 days of wound induction. Figure 8L shows newly formed surface epithelium over the scar tissue, in diabetic group received nitric oxide donor nanoparticles after 14 days of wound induction.

Figure 8: Histological examination of wound with topical application of nitric oxide-releasing nanoparticles. (A-L) Cross-section of representative histology images of H&E and Trichrome staining at 3,7 and 14 days of wound induction.



Scoring analysis of skin wound

Table (1) shows scoring of **acute changes of skin wounds** for all groups at the 3rd, 7th and 14th day of wound induction.

The control group showed maximum score on the 3rd day of wound induction followed by a decreased on the 7th day and totally disappeared in the 14th day of wound induction. The control group received NONPs showed insignificant difference in acute changes as compared with control group.

Diabetic mice showed significant increase in acute parameters as compared with control group on the 7th day of wound induction, however on the 14th day insignificant change observed as compared to control group.

The diabetic group received nitric oxide donor nanoparticles showed no significant difference as compared with control group throughout the whole experiment period, however significant decrease in acute parameters observed as compared to diabetic group in the 7th day of wound induction.

Table (2) shows scoring of **regenerative changes of skin wounds** for all groups at the 3rd, 7th and 14th day of wound induction.

As regard to control group, the 3rd day of wound induction the evidence of regeneration represented in capillaries and fibroblast formation. On the 7th day surface epithelium cells began to proliferate to cover the wound with the proliferation of capillaries and fibroblast in the interface area. After 14 days remodeling of the epithelial covering began with mild decrease in the number of layers and increase in capillaries and fibroblast. Collagen bundles become more dense and thick with complete disappearance in hair follicles and sweat glands. Control group received NONP showed similar events as compared to control group.

On the other hand, for diabetic group on the 3rd and 7th days of wound induction the regenerative changes were delayed and manifested by decreased number of regenerative epithelium and delay in capillaries formation and fibroblast proliferation in the interface area which made significant difference in regenerative changes in diabetic group verses control group.

Diabetic group received NONPs recorded marked delayed onset of regeneration on the 3rd day of wound induction compared to control group, however regenerating parameters were similar to control group on the 7th and 14th day of wound induction. In addition, the treated diabetic group also scored significant increase in regenerating parameters as compared to diabetic group on the 7th day of wound induction.

Table (3) display scoring of healed fibrotic changes of skin wounds for all groups on the 3rd, 7th and 14th day of wound induction.

In control group the nerve bundles are pulled upward from the depth of the wound by the effect of retraction of the formed collagen bundles. On the 3rd day collagen matrix began to develop in the wound gap and get thicker on the 7th and 14th day post wounding with complete disappearance of hair follicles and rete ridges. The same results were observed in control group received nitric oxide donor nanoparticles.

As regard to diabetic group, collagen bundles formation were deficient on the 3rd and 7th days of wound induction to be postponed to the 14th day of wound induction. By the 14th day post wounding thick collagen bundles was formed.

Diabetic group received NONPs showed no significant difference as compared to control group; however it showed significant difference in the formation of collagen bundles on the 3rd and 7th day after wound induction.

Table 1: Scoring of acute changes (Ulcerated with crust, Neutrophils and Hyaline fibrinoid material) of cutaneous wounds healing after topical application of nitric oxide-releasing nanoparticles at 3, 7 and 14 days after wound induction based on the histological examination.

	Acute changes											
	Control			CNOp			Diabetic			DNOp		
	3rd day	7 th day	14th day	3rd day	7 th day	14th day	3rd day	7 th day	14th day	3rd day	7 th day	14th day
1) Surface epithelial changes												
Ulcerated with crust	10	0	0	10	0	0	10	10	0	10	10	0
Neutrophils	10	10	0	20	10	0	10	10	0	10	0	0
Hyaline fibrinoid material	0	0	0	0	0	0	10	10	0	10	0	0
2)The wound gap												
Necrotic tissue	10	0	0	10	0	0	10	0	0	10	0	0
Density of Neutrophils	10	10	0	10	10	0	10	20	0	10	10	0
3) Interface area with the non-injured tissues												
Neutrophils	10	0	0	10	10	0	10	10	0	10	10	0
Total Score	50	20	0	60	30	0	60	60*	0	60	30*	0

*= significance as compared with control group

•= significance as compared with diabetic group

Table 2: Scoring of regenerative changes of cutaneous wounds after topical application of nitric oxide-releasing nanoparticles at 3, 7 and 14 days after wound induction based on the histological examination.

	Regenerative changes											
	Control			CNOnp			Diabetic			DNOnp		
	3 rd day	7 th day	14 th day	3 rd day	7 th day	14 th day	3 rd day	7 th day	14 th day	3 rd day	7 th day	14 th day
Surface epithelial changes												
No. of rows	0	30	20	0	30	20	0	10	20	0	30	20
Rete ridges	0	0	10	0	0	10	0	0	0	0	0	0
The wound gap												
Capillaries	10	10	10	0	10	10	0	10	10	0	10	10
Fibroblast	10	10	10	0	10	10	0	10	10	0	10	10
Hair follicles	0	0	0	0	0	0	0	0	0	0	0	0
Sweet glands	0	0	0	0	0	0	0	0	0	0	0	0
Interface area with the non-injured tissues												
Capillaries	0	10	0	10	10	0	0	0	10	0	10	10
Fibroblast	0	10	10	10	10	0	0	0	10	0	10	10
Hair follicles	0	0	0	0	0	0	0	0	0	0	0	0
Sweet glands	0	0	0	0	0	0	0	0	0	0	0	0
Total score	20	70	60	20	70	50	0*	30*	60	0*	70*	60

* significance as compared with control group
 ● significance as compared with diabetic group

Table 3: Scoring of healed fibrotic changes of cutaneous wounds after topical application of nitric oxide-releasing nanoparticles at 3, 7 and 14 days after wound induction based on the histological examination.

	Healed Fibrotic changes											
	Control			NONPs			Diabetic			Diabetic+ NONPs		
	3 rd day	7 th day	14 th day	3 rd day	7 th day	14 th day	3 rd day	7 th day	14 th day	3 rd day	7 th day	14 th day
1) The wound gap												
Collagen matrix	10	10	10	0	10	10	0	0	10	0	10	10
Nerve bundles	10	0	10	0	0	10	0	0	10	10	10	0
2) Interface area with the non-injured tissues												
Collagen matrix	0	10	10	10	10	10	0	0	10	0	10	10
Nerve bundles	0	10	0	10	0	0	0	0	0	10	10	0
Total score	20	30	30	20	20	30	0*	0*	30	20*	40*	20

* significance as compared with control group

● significance as compared with diabetic group

DISCUSSION

The NO-releasing hydrogel nanoparticles were based on a combination of polymers including low molecular weight chitosan and PEG in addition to TMOS and glucose, and using sodium nitrite as the NO-precursor. The glucose role was to confer a thermal reduction of the loaded NO-donor, sodium nitrite, to generate NO gas. The resulting NO gas remains entrapped inside the developed hydrogel nanoparticles until undergoing a sustained release due to the swelling of the hydrogel nanoparticles in moist environments.

In the present study, the chitosan IR spectrum demonstrated a peak at about 3342 cm^{-1} which was assigned for the N-H extension vibration, the O-H stretching vibration, and the H-bonding of the polysaccharide moieties of the chitosan polymer. The peak noted at 2883 cm^{-1} was assigned for the stretching vibrations of the C-H (aliphatic) bonds whereas, the absorption signal noted at 1590 cm^{-1} was attributed to the stretching vibration of amide C=O bonds.

TEM images of the prepared NONPs revealed a spherical morphology with uniformed particle size mostly below 50nm. NO was released from the NONPs in a sustained manner without burst release upon the addition of the hydrogel nanoparticles to the PBS buffer at pH 7.1. The NO release study was performed at pH7.1 since wound pH can decrease during the course of healing [23]. This is reflected on the NO levels in wound tissue when NONPS bandage was applied on wound. Compared to wound of control mice, there was remarkable high NO levels in wound tissue in NONPS bandage applied to wound in control and diabetic treated mice. Since increasing the initial concentration of the nanoparticles demonstrated a significant increase in the released NO (nM) at any time interval NO release from NONPs could be further optimized.

Wound healing is impaired in diabetes and NO enhances wound healing efficacy in several conditions [24, 25]. However progress of wound healing treatment is slow due to insufficient NO delivery system. The gaseous state and short half-life of NO require a platform-based formula that can regulate its storage and release [24]. In addition, wound healing is hampered by increased oxidative stress with decrease vascularization due to poor angiogenesis [26]. Nanoparticles can be useful in drug delivery due their physiochemical properties that enable to overcome biomedical and biophysical barrier and improve pharmacological and therapeutic outcomes [9]. In this study, NO releasing bandage composed of sodium nitrite as NO donor in nanoformulation was developed for wound healing in diabetics that is effective and easy to apply. In the present study, wound area in diabetic mice treated with NONPs bandage showed significant decrease compared with diabetic non treated mice indicating improvement of wound healing process.

Oxidative stress has been shown to be detrimental to multiple cellular processes in wound healing. There were significantly reduced levels of NO and GSH as well as SOD and CAT activities in diabetic wounds, with increased MDA production due to lipid peroxidation. Reactive oxygen specie (ROS) such as superoxide and hydroxyl radicals are continuously generated in human tissue and over production induced oxidative cellular injury that contributes to wound worsening [27]. Wound tissue from diabetic mice demonstrated remarkable decrease in NO and antioxidants which could indicate an increase in ROS production that could reduce the antioxidant capacity and aggravate the wound. The interaction between superoxide radical and nitric oxide can form harmful peroxynitrite that cause nitroxidation of protein and intensify wound complication [28]. Therefore, it is hypothesized that antioxidants are required to protect tissue from oxidative injury and improve wound healing. Topical application of NONPs bandage increased cutaneous NO and GSH levels as well as SOD, CAT activities with concomitant suppression lipid peroxidation. This effect hampered the adverse effect of ROS which reflected on wound closure area that demonstrated remarkable decrease. In addition, decreased lipid peroxidation could reduce the interaction between MDA and DNA bases and prevent mutagenic lesions[29]. Interestingly, NO can show antioxidant potential since it is vital in setting precise homeostasis of superoxide/nitric oxide and inhibiting xanthine oxidase [30]. This ratio is essential for setting effective strategy in therapy of diabetic skin [31]

In addition the VEGF and TGF-B1 have increased markedly in wound tissues. VEGF directly activated NOS, which would lead to an increase in NO production and stimulates endothelial cell (EC) migration [32]. The NO released from the bandage serve to protect wound tissue by signaling and improving blood flow and inhibiting thrombosis and accumulation of enzymes that mediate cellular destruction [25]. NO also showed an antimicrobial influence including viruses, bacteria, fungi and parasites [25].

The formation of fibroblast is the hallmark of wound healing [33]. The histopathological results showed that more abundant inflammatory cells and fibroblast formation was observed in the area dressed with NONPs (Figure 8). This leads to a healing process faster than the diabetic animals. It appeared that the prepared NONPs bandage promotes the tensile strength of tissue by accelerating the formation of fibroblasts and the synthesis of collagen in the first few days of wound healing. Fibroblasts can provide new fibers and ground substance to replace the injured areas. This agrees with finding that these fibroblast formations induced angiogenesis and collagen formation in the wounded area [33]. This is supported by newly formed capillaries in regenerating epithelium and fibroblast within collagen bundles in diabetic group received NONPs after 7 days of wound induction. In addition, re-epithelialization is seen in NONPs bandage applied on wound of diabetic animals. Newly formed surface epithelium over the scar tissue, wound fibrous tissue and nerve bundles in diabetic group received NONPs after 14 days of wound induction was observed.

The data suggest that NONPs is a potential treatment for wound dressing. These bandages are easy to fabricate thus making them an attractive option for use in homes and clinical practice.

REFERENCES

- [1] Park, N.Y. and Y. Lim, Short term supplementation of dietary antioxidants selectively regulates the inflammatory responses during early cutaneous wound healing in diabetic mice. *Nutr Metab (Lond)*, 2011. 8(1): p. 80.
- [2] Zheng, Y., et al., Topical administration of cryopreserved living micronized amnion accelerates wound healing in diabetic mice by modulating local microenvironment. *Biomaterials*, 2017. 113: p. 56-67.
- [3] Ricco, J.B., et al., The diabetic foot: a review. *J Cardiovasc Surg (Torino)*, 2013. 54(6): p. 755-62.
- [4] Nakagami, H., et al., Endothelial dysfunction in hyperglycemia as a trigger of atherosclerosis. *Curr Diabetes Rev*, 2005. 1(1): p. 59-63.
- [5] Boykin, J.V., Jr., Wound nitric oxide bioactivity: a promising diagnostic indicator for diabetic foot ulcer management. *J Wound Ostomy Continence Nurs*, 2010. 37(1): p. 25-32; quiz 33-4.
- [6] Pitocco, D., et al., Oxidative stress, nitric oxide, and diabetes. *Rev Diabet Stud*, 2010. 7(1): p. 15-25.
- [7] Mikaili, P., M. Moloudizargari, and S. Aghajanshakeri, Treatment with topical nitroglycerine may promote the healing process of diabetic foot ulcers. *Med Hypotheses*, 2014. 83(2): p. 172-4.
- [8] Durmus, A.S., et al., Arginine Silicate Inositol Complex Accelerates Cutaneous Wound Healing. *Biol Trace Elem Res*, 2016.
- [9] Das, S. and A.B. Baker, Biomaterials and Nanotherapeutics for Enhancing Skin Wound Healing. *Front Bioeng Biotechnol*, 2016. 4: p. 82.
- [10] Wang, E.C. and A.Z. Wang, Nanoparticles and their applications in cell and molecular biology. *Integr Biol (Camb)*, 2014. 6(1): p. 9-26.
- [11] Quinn, J.F., M.R. Whittaker, and T.P. Davis, Delivering nitric oxide with nanoparticles. *J Control Release*, 2015. 205: p. 190-205.
- [12] Li, Y. and P.I. Lee, Controlled nitric oxide delivery platform based on S-nitrosothiol conjugated interpolymer complexes for diabetic wound healing. *Mol Pharm*, 2010. 7(1): p. 254-66.
- [13] Friedman, A.J., et al., Sustained release nitric oxide releasing nanoparticles: characterization of a novel delivery platform based on nitrite containing hydrogel/glass composites. *Nitric Oxide*, 2008. 19(1): p. 12-20.
- [14] Trinder, P., Determination of glucose in blood using glucose oxidase with an alternative oxygen acceptor. *Annals of Clinical Biochemistry: An international journal of biochemistry in medicine*, 1969. 6(1): p. 24-27.
- [15] Montgomery, H. and J. Dymock, Colorimetric determination of nitric oxide. *Analyst*, 1961. 86(4): p. 4.
- [16] Ohkawa, H., N. Ohishi, and K. Yagi, Assay for lipid peroxides in animal tissues by thiobarbituric acid reaction. *Analytical biochemistry*, 1979. 95(2): p. 351-358.
- [17] Prins, H. and J. Loos, Glutathione, in *Biochemical methods in red cell genetics* 1969, Academic Press New York. p. 115-137.
- [18] Nishikimi, M., N.A. Rao, and K. Yagi, The occurrence of superoxide anion in the reaction of reduced phenazine methosulfate and molecular oxygen. *Biochemical and biophysical research communications*, 1972. 46(2): p. 849-854.
- [19] Böck, P., et al., Peroxisomes and related particles in animal tissues. Vol. 7. 1980: Springer.
- [20] Basu, S., et al., The neurotransmitter dopamine inhibits angiogenesis induced by vascular permeability factor/vascular endothelial growth factor. *Nature medicine*, 2001. 7(5): p. 569-574.

- [21] Sporn, M.B., et al., Transforming growth factor-beta: biological function and chemical structure. *Science*, 1986. 233(4763): p. 532-534.
- [22] Bancroft, J. and A. Stevens, Mounting media. Theory and practice of histological techniques. New York: Churchill Livingstone. p, 1996. 735.
- [23] Gethin, G., The significance of surface pH in chronic wounds. *Wounds uk*, 2007. 3(3): p. 52.
- [24] Kim, J.O., et al., Nitric oxide-releasing chitosan film for enhanced antibacterial and in vivo wound-healing efficacy. *Int J Biol Macromol*, 2015. 79: p. 217-25.
- [25] Lowe, A., et al., Electrospun nitric oxide releasing bandage with enhanced wound healing. *Acta Biomater*, 2015. 13: p. 121-30.
- [26] Ganzarolli de Oliveira, M., S-Nitrosothiols as Platforms for Topical Nitric Oxide Delivery. *Basic & clinical pharmacology & toxicology*, 2016.
- [27] Pessoa, A.F., et al., Oral administration of antioxidants improves skin wound healing in diabetic mice. *Wound Repair Regen*, 2016.
- [28] Fadini, G.P., et al., The redox enzyme p66Shc contributes to diabetes and ischemia-induced delay in cutaneous wound healing. *Diabetes*, 2010. 59(9): p. 2306-14.
- [29] Goncalves, R.V., et al., 5alpha-Dihydrotestosterone enhances wound healing in diabetic rats. *Life Sci*, 2016. 152: p. 67-75.
- [30] Arcaro, A., et al., Novel Perspectives in Redox Biology and Pathophysiology of Failing Myocytes: Modulation of the Intramyocardial Redox Milieu for Therapeutic Interventions-A Review Article from the Working Group of Cardiac Cell Biology, Italian Society of Cardiology. *Oxid Med Cell Longev*, 2016. 2016: p. 6353469.
- [31] Jankovic, A., et al., Targeting the superoxide/nitric oxide ratio by L-arginine and SOD mimic in diabetic rat skin. *Free Radic Res*, 2016. 50(sup1): p. S51-S63.
- [32] Dimmeler, S., E. Dernbach, and A.M. Zeiher, Phosphorylation of the endothelial nitric oxide synthase at ser-1177 is required for VEGF-induced endothelial cell migration. *FEBS Lett*, 2000. 477(3): p. 258-62.
- [33] Azad, A.K., et al., Chitosan membrane as a wound-healing dressing: characterization and clinical application. *J Biomed Mater Res B Appl Biomater*, 2004. 69(2): p. 216-22.